

Electronic Supporting Information
for
Triphenylphosphonium conjugated quaternary ammonium based gel: synthesis and
potential application in efficient removal of toxic acid orange 7 dye from aqueous
solution

Sayantani Bhattacharya, Diptendu Patra and Raja Shunmugam*

Polymer Research Centre, Department of Chemical Sciences and Centre for Advanced
Functional Materials, Indian Institute of Science Education and Research Kolkata, Mohanpur,
West Bengal, 741246, India

*E-mail: sraja@iiserkol.ac.in

Sl no.	Contents	Page no.
1	Experimental Section	S3
2	Figure S1: ¹ H NMR spectrum of compound 3	S5
3	Figure S2: ¹ H NMR spectrum of compound 4	S5
4	Figure S3: ¹³ C NMR spectrum of compound 4	S6
5	Figure S4: ESI-MS of compound 4	S6
6	Figure S5: ¹ H NMR spectrum of compound 5	S7
7	Figure S6: ¹³ C NMR spectrum of compound 5	S7
8	Figure S7: ³¹ P NMR spectrum of compound 5	S8
9	Figure S8: ESI-MS of compound 5	S8
10	Figure S9: ¹ H NMR spectrum of compound 6	S9
11	Figure S10: ¹³ C NMR spectrum of compound 6	S9
12	Figure S11: ³¹ P NMR spectrum of compound 6	S10
13	Figure S12: ESI-MS of compound 6	S10
14	Figure S13: Differential Scanning Calorimetry of TPP gel for a) heating and b) cooling cycle respectively.	S11
15	Figure S14: FE-SEM image of as prepared TPP gel	S11
16	Figure S15: Hansen solubility parameter of the solvents	S12

	used.	
16	Figure S16: pHzpc data of the TPP gel.	S12
17	Equation S1: Formula for dye adsorption	S13
18	Table S1. Adsorption capacity of different chemical adsorbents for the removal of azo dyes as recognised by their maximum adsorption capacity (mg of dye/g of adsorbent)	S13
19	Table S2. Adsorption capacity of different bio-adsorbents for the removal of azo dye acid orange 7 as recognised by their maximum adsorption capacity (mg of dye/g of adsorbent)	S14
20	References	S14

Experimental Section:

Instrumentation Techniques:

Nuclear Magnetic Resonance (NMR): The ^1H , ^{13}C and ^{31}P NMR spectroscopy was carried out on a BRUKER 500 MHz spectrometer using CDCl_3 , $\text{DMSO}-d_6$, and D_2O as solvents. ^1H NMR spectra were calibrated to tetramethylsilane as internal standard (δ_{H} 0.00).

Fourier Transform Infra -Red (FT-IR): FT-IR spectra were obtained on FT-IR Perkin-Elmer spectrometer at a nominal resolution of 2 cm^{-1} .

ESI-MS: HRMS analyses were performed with Q-TOF YA263 high resolution (Waters Corporation) instruments by +ve mode electrospray ionization.

Rheometer: The rheological measurements were carried out on a TA-ARG2 rheometer using a steel parallel plate with 60 mm diameter at $25\text{ }^\circ\text{C}$ with 1.0 mm Gap spacing for all gel samples. The dynamic shear moduli (G' and G'') were recorded in the linear viscoelastic regime at a strain of $\gamma = 1\%$ as a function of angular frequency (0.1–100 rad/s).

UV-Vis Spectroscopy: UV-visible absorption measurements were carried out on U-4100 spectrophotometer; HITACHI spectrometer, with a scan rate of 500 nm/min.

Scanning Electron Microscopy (SEM): High resolution SEM was performed on a Zeiss microscope; SUPRA 55VP-Field Emission Scanning Electron Microscope. High performance variable pressure FE-SEM with patented GEMINI column technology. Schottky type field emitter system, single condenser with crossover-free beam path. Resolution: 1.0 nm at 15 kV; 1.6 nm at 1 kV high vacuum mode. 2.0 nm at 30 kV at variable pressure mode.

Thermo Gravimetric Analysis: Thermal studies were carried out using a Mettler Toledo TGA/SDTA 851e instrument at a heating rate of $10\text{ }^\circ\text{C min}^{-1}$.

Transmission Electron Microscopy:

The gels were sliced at 30 nm thick films using microtome facility (Power Tome PC, RMC Boeckeler). The sliced film was dried under vacuum and was analysed using Transmission Electron Microscope; TEM (JEM-2100F) facility at 120 kV.

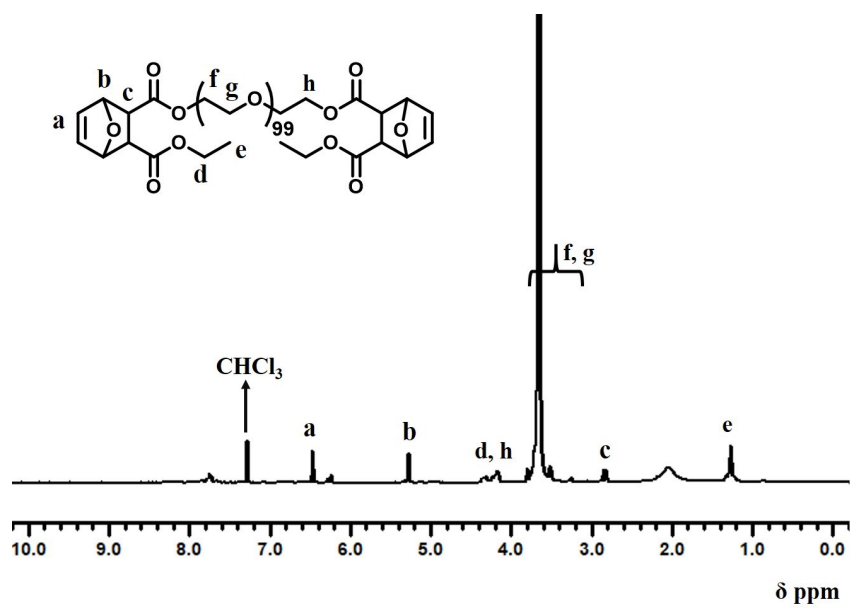


Figure S1: ^1H NMR spectrum of compound 3 in CDCl_3

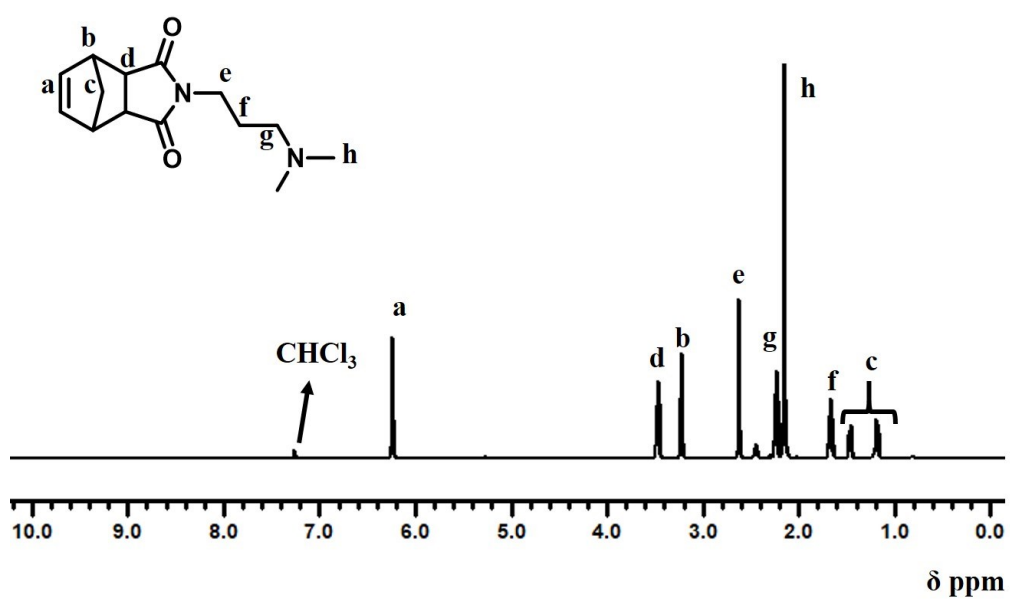


Figure S2: ^1H NMR spectrum of compound 4 in CDCl_3

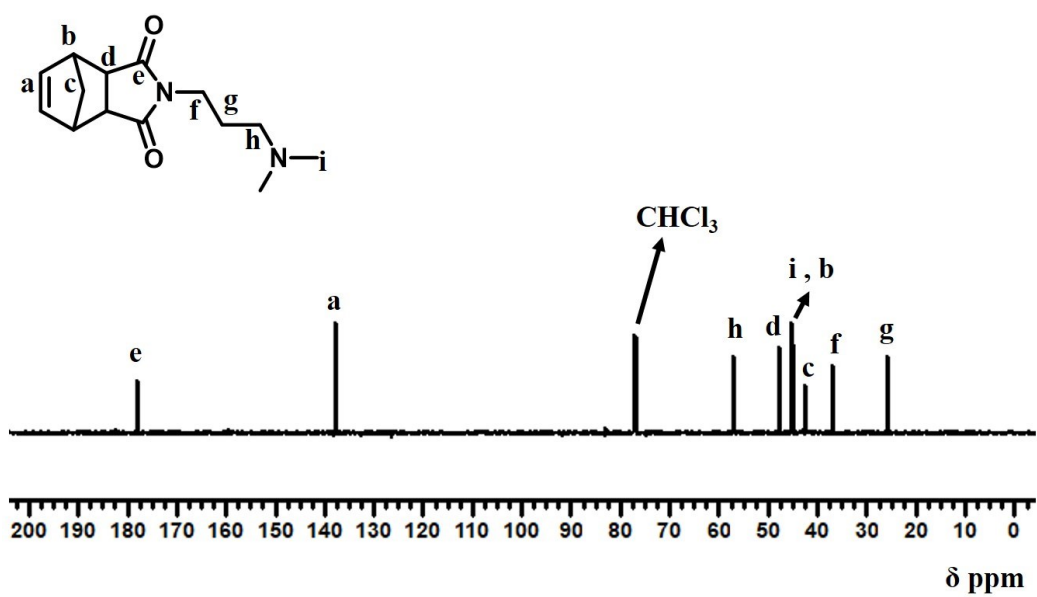


Figure S3: ^{13}C NMR spectrum of compound 4 in CDCl_3

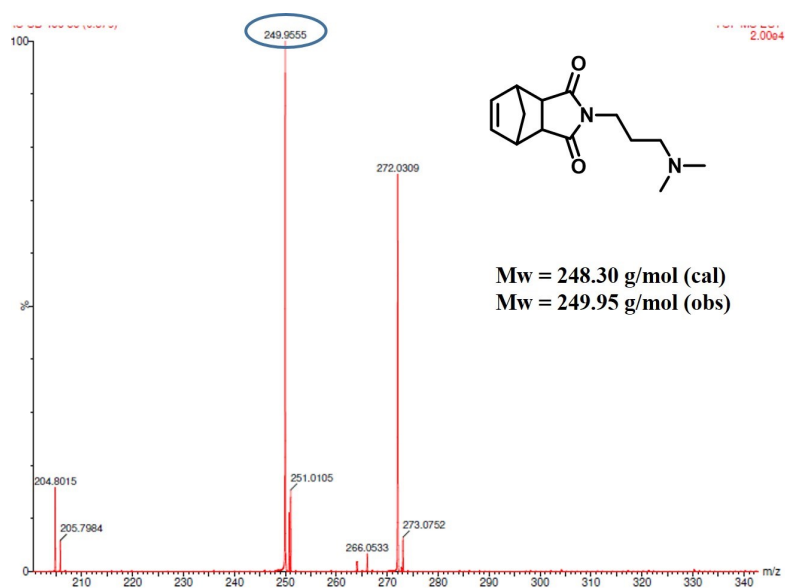


Figure S4: ESI-MS of compound 4 confirming its formation

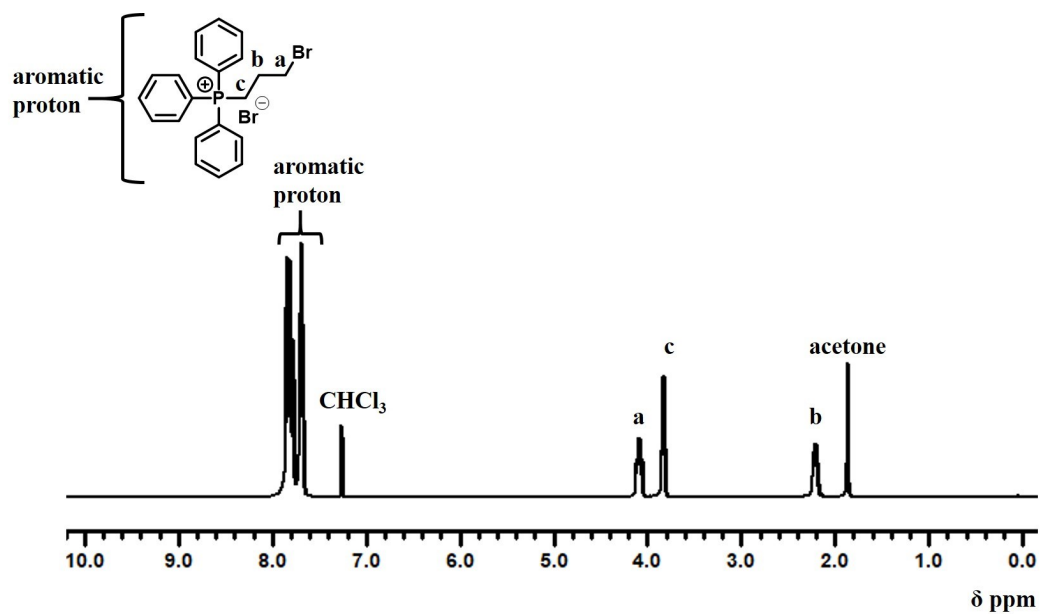


Figure S5: ^1H NMR spectrum of compound 5 in CDCl_3

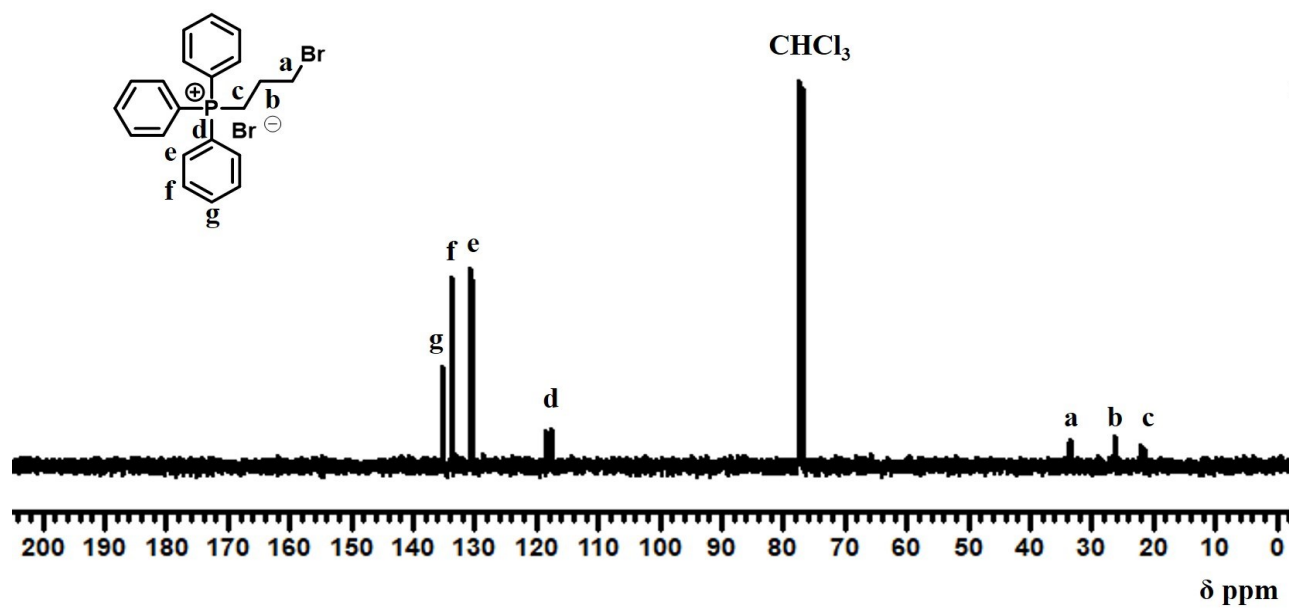


Figure S6: ^{13}C NMR spectrum of compound 5 in CDCl_3

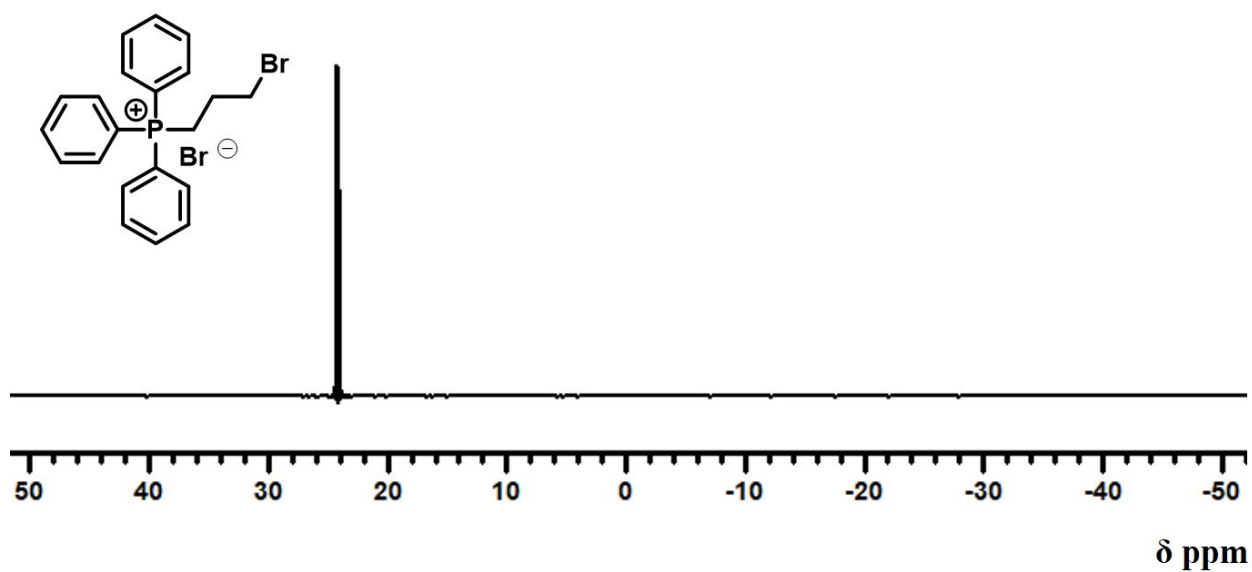


Figure S7: ^{31}P NMR of compound 5 in CDCl_3

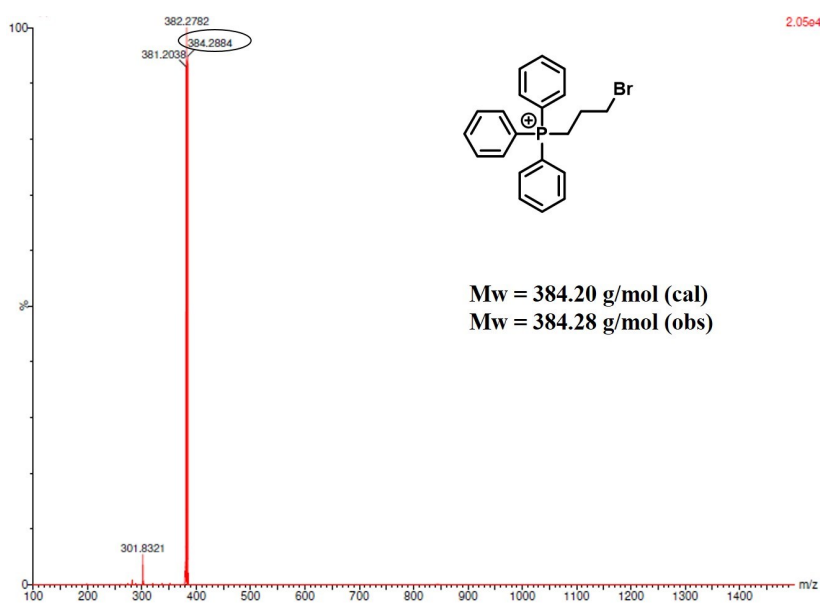


Figure S8: ESI-MS of compound 5 confirming its formation

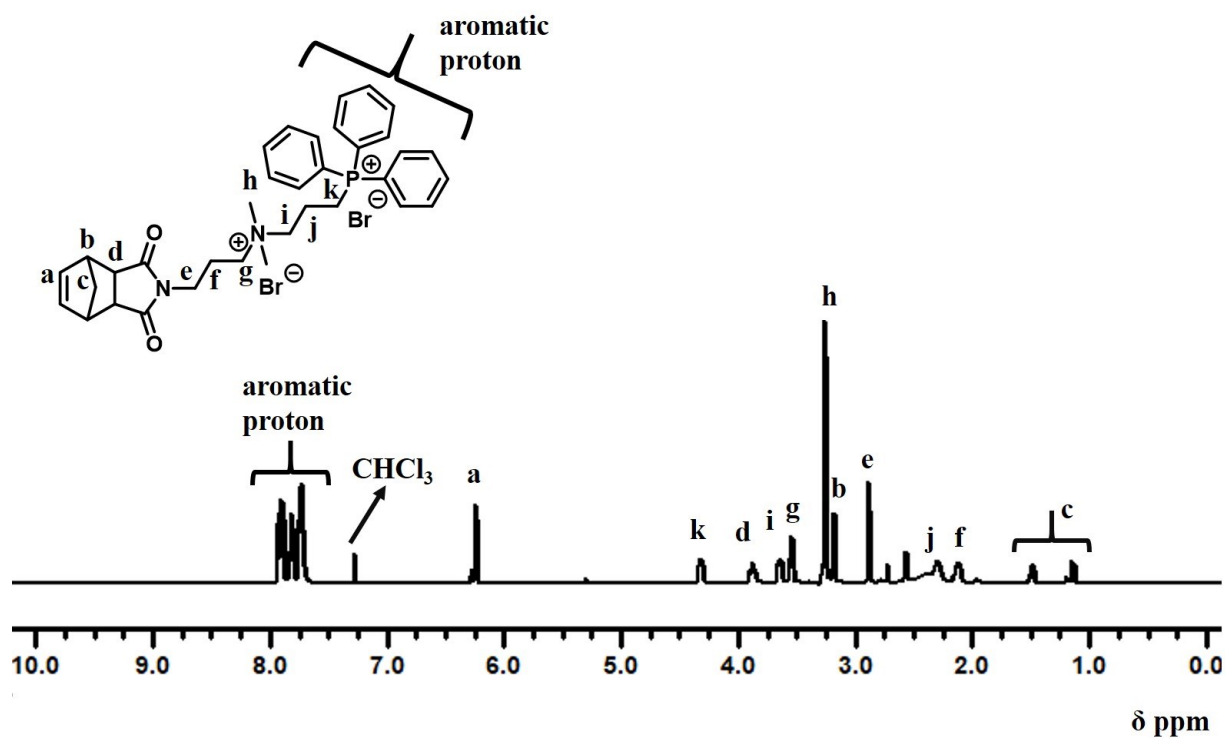


Figure S9: ^1H NMR spectrum of compound 6 in CDCl_3

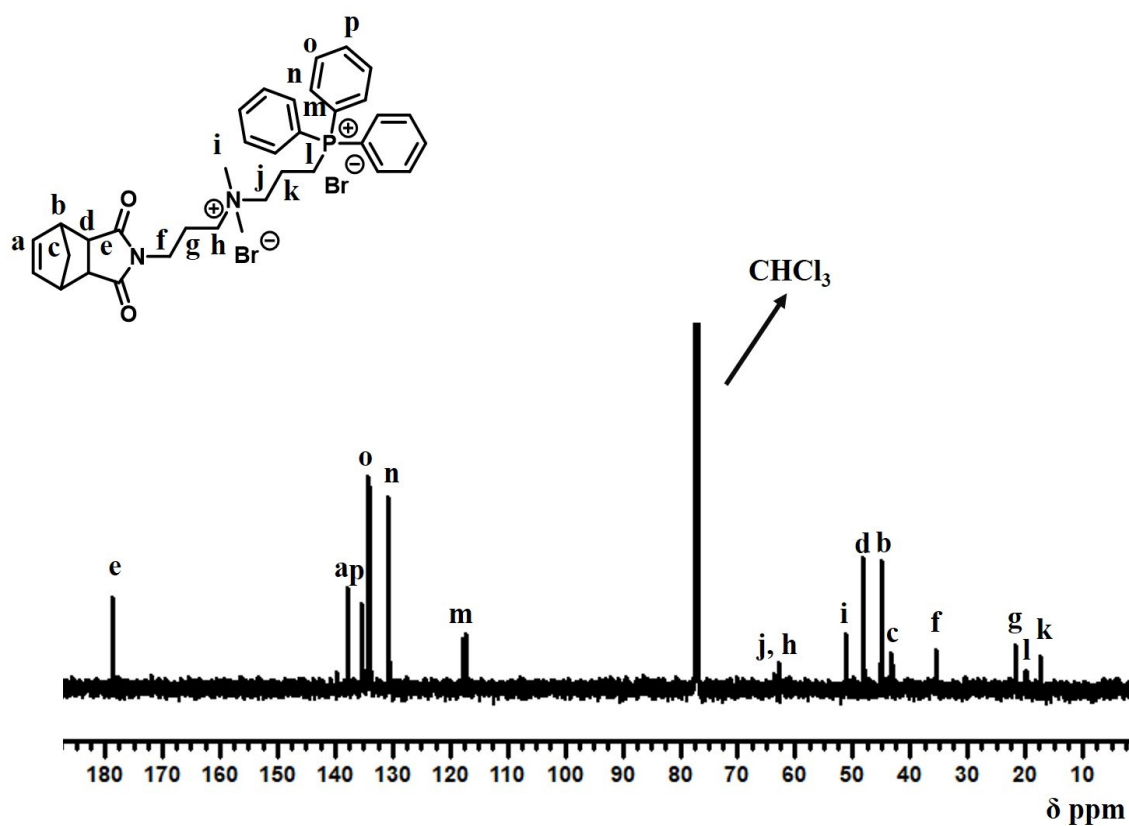


Figure S10: ^{13}C NMR spectrum of compound 6 in CDCl_3

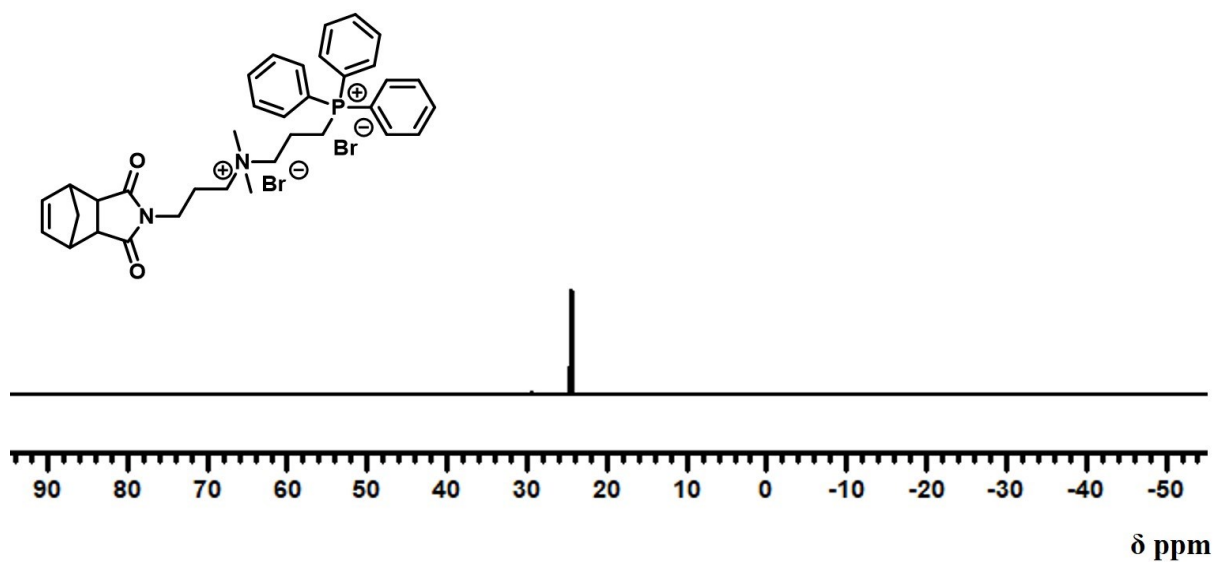


Figure S11: ^{31}P NMR of compound 6 in CDCl_3

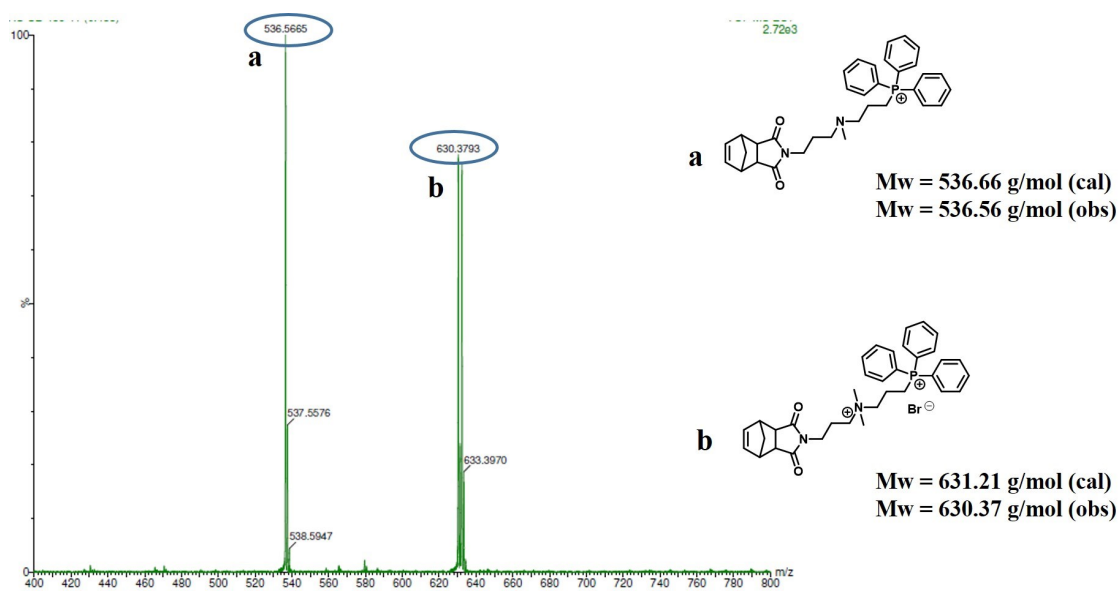


Figure S12: ESI-MS of compound 6 confirming its formation

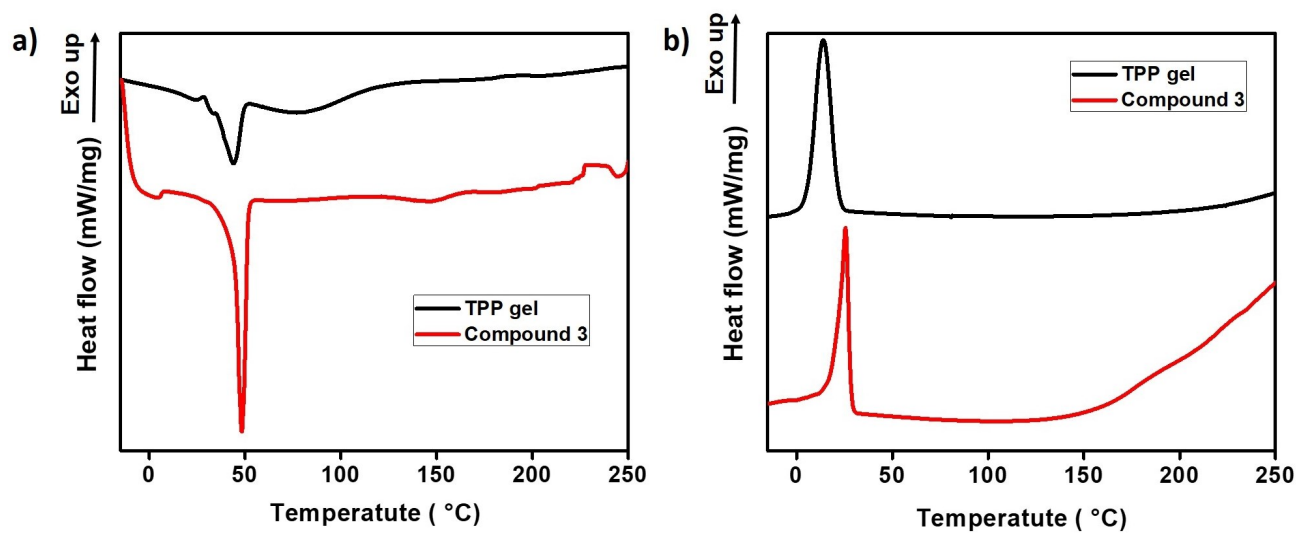


Figure S13: Differential Scanning Calorimetry of Compound 3 and TPP gel for a) heating and b) cooling cycle respectively.

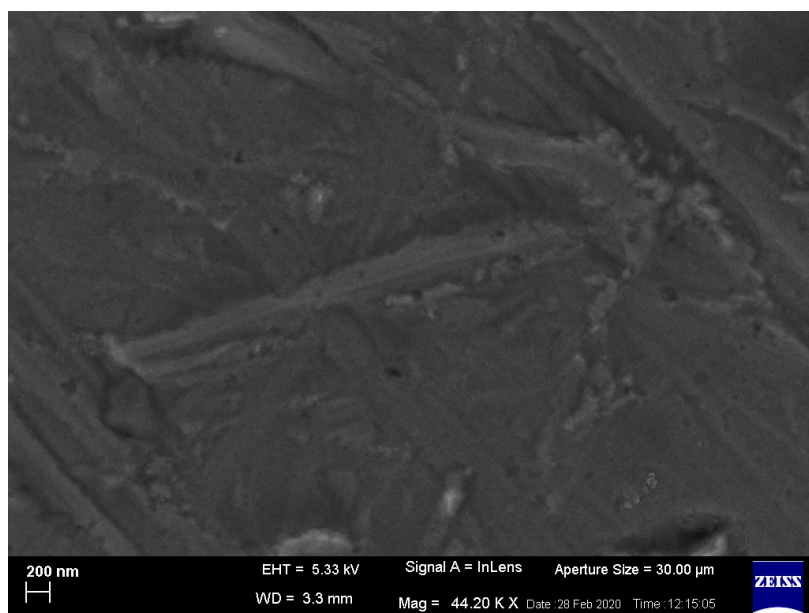


Figure S14: FE-SEM image of the as prepared TPP gel.

Solvent	Solubility parameter, $\delta_{\text{solvent}} \text{ (cal cm}^{-3}\text{)}^{1/2}$
Water	23.40
DMSO	13.03
DMF	12.14
1,4- dioxane	10.02
DCM	9.93
THF	9.52

Figure S15: Hansen solubility parameter of the solvents used.

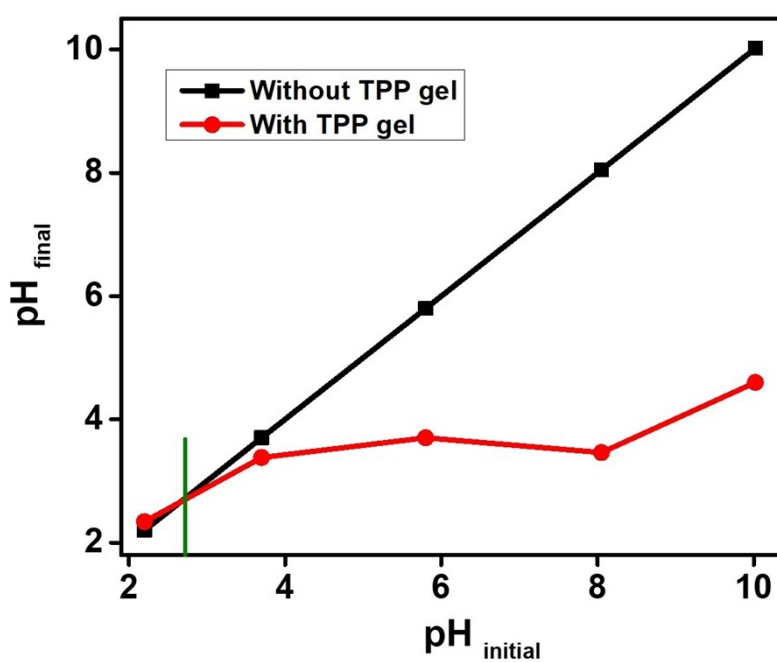


Figure S16: pHzpc data of the TPP gel.

Equation S1: Formula for dye adsorption

$$\text{dye removal (\%)} = \frac{C_0 - C_t}{C_0} \times 100$$

where C_0 (mg/L) and C_t (mg/L) represent the initial and final (or at time t) concentration of dye in aqueous solution.

Table S1. Adsorption capacity of different chemical adsorbents for the removal of azo dyes as recognised by their maximum adsorption capacity (mg of dye/g of adsorbent)

Adsorbent	Dye sorbate	Maximum removal efficiency (mg/g)	Reference
Granular activated carbon	Congo red	9.1	1
Zeolite	DB 71	13.7	2
Graphene oxide	acid orange 8	29.0	3
Cellulose/chitosan hydrogel	Congo red	40	4
Chitosan halloysite nanotubes	Congo red	41.5	5
Magnetic graphene/chitosan (MGCh) nanocomposite	Acid orange 7	42.7	6
Chemically modified brown macroalga	Acid orange 2	45.47	7
Amberlite IRA-958	Acid orange 7	50	8
Multiwalled carbon nanotube	tartrazine	84.0	9
Thiol-norbornene based photo crosslinked network	Acid orange 7	98.6	This work
Graphitized and heteroatom doped porous carbon	Acid orange 7	285.71	10

Table S2. Adsorption capacity of different bio-adsorbents for the removal of azo dye acid orange 7 as recognised by their maximum adsorption capacity (mg of dye/g of adsorbent)

Adsorbent	Dye sorbate	Maximum removal efficiency (mg/g)	Reference
PR leaves	Acid orange 7	7.52	11
Paulownia tomentosa Steud leaf powder	Acid orange 52	10.5	12
Canola stalks (CS)	Acid orange 7	25.06	13
Spent brewery grains	Orange II	28.54	14
Brown macro alga <i>Stoechospermum marginatum</i>	Acid orange 7	35.62	15

References:

- 1 D. Olivo-Alanis, R. B. Garcia-Reyes, L. H. Alvarez and A. Garcia-Gonzalez, *J. Hazard. Mater.*, 2018, **347**, 423.
- 2 N. Mirzaei, A. H. Mahvi and H. Hossini, *Adsorpt. Sci. Technol.*, 2018, **36**, 80.
- 3 W. Konicki, M. Aleksandrak, D. Moszyński and E. Mijowska, *J. Colloid Interface Sci.*, 2017, **496**, 188.
- 4 M. Li, Z. Wang and B. Li, *Desalin. Water Treat.*, 2016, **57**, 16970.
- 5 S. Vahidhabanu, A. I. Adeogun and B. R. Babu, *ACS Omega*, 2019, **4**, 2425.
- 6 S. Sheshmani, A. Ashori and S. Hasanzadeh, *Int. J. Biol. Macromol.*, 2014, **68**, 218.
- 7 M. Kousha, E. Daneshvar, M. S. Sohrabi, M. Jokar and A. Bhatnagar, *Chem. Eng. J.*, 2012, **192**, 67.
- 8 M. Greluk and Z. Hubicki, *Desalination*, 2011, **278**, 219.

- 9 J. Goscianska and R. Pietrzak, *Catal. Today*, 2015, **249**, 259.
- 10 Z. Liu, F. Zhang, T. Liu, N. Peng and C. Gai, *J. Environ. Manage.*, 2016, **182**, 446.
- 11 R. Rehman, S. J. Muhammad and M. Arshad, 2019, 1.
- 12 F. Deniz and S. D. Saygideger, *Bioresour. Technol.*, 2010, **101**, 5137.
- 13 Y. Hamzeh, A. Ashori, E. Azadeh and A. Abdulkhani, *Mater. Sci. Eng. C*, 2012, **32**, 1394.
- 14 E. R. García, R. L. Medina, M. M. Lozano, I. H. Pérez, M. J. Valero and A. M. Maubert Franco, *Materials (Basel)*, 2014, **7**, 8037.
- 15 M. Kousha, E. Daneshvar, M. S. Sohrabi, M. Jokar and A. Bhatnagar, *Chem. Eng. J.*, 2012, **192**, 67.